PIER C

(Received 20 December 2025, Accepted 30 March 2026, Scheduled 20 June 2026)

Effect of Changing Polynomial Parameters of Vortex Laguerre Beam on Behavior of Symbol Error Rate

Ali A. Dheyab[1], Asmaa M. Aubaid[2,*], Ekhlas K. Hamza[3], and Hamid Sh. Aldulaimi[4]

[1] *Department of Electronics and Communication Engineering, University of Al-Nahrain, Baghdad, Iraq*
[2] *Scientific Research Commission, Baghdad, Iraq*
[3] *College of Artificial Intelligence Engineering, University of Technology, Baghdad, Iraq*
[4] *Ministry of Higher Education and Scientific Research, Iraq*

ABSTRACT: In optical communications, symbol error rate (SER) is a key indicator of system performance when data is transmitted over optical channels. Improving this rate is a major goal in the design of advanced optical systems, as many factors affect performance, including noise and optical impairments. One mathematical method proven effective for improving performance is the use of Laguerre polynomials. This study investigates the impact of variations in the polynomial parameters regarding Laguerre-Gaussian vortex beam (LGVB) on symbol error rate (SER) under weak, moderate, and strong turbulence conditions. The research uses numerical simulations to analyze the beam's intensity profiles and SER for various parameter combinations. Key findings show that specific parameter pairs yield superior SER performance, reducing error rates. The lowest SER under high turbulence is observed at $(3, 0)$ and $(2, 0)$ due to their spatially dispersed intensity profiles. Optimizing LGVB's polynomial parameters enhances SER robustness in turbulent FSO systems, offering a practical, non-hardware-based mitigation strategy. Simulation results for ($n = 3$, $m = 0$) show that the proposed beam configuration reduces SER to the minimum value compared to other Laguerre Gaussian Vortex beams with different values of radial index (n) and topological charge (m) under identical turbulence conditions ($Cn^2 = 10^{-12}m^{-\frac{2}{3}}$). This work provides actionable insights for designing turbulence-resilient optical links, particularly in satellite-to-ground and long-range terrestrial communications.

1. INTRODUCTION

We classify the literature into three groups. The first group concerns adaptive optics (AO) systems, which use wavefront sensing and correction to compensate for disturbances [1, 2]. Mackey and Denty [3] showed that adaptive optics (AO) works well in situations with high turbulence, characterized by changes in light intensity, while Schwartz et al. [4] highlighted the challenges of correcting phase changes when disturbances vary in strength. However, AO systems face practical limitations, including aperture-size constraints [5] and cost-complexity trade-offs [6]. When it comes to modulation and detection methods, coherent detection with advanced modulation schemes, such as Amplitude Shift Keying (ASK) by changing the intensity or amplitude of the optical signal, Phase Shift Keying (PSK) by changing the phase of the light wave, Frequency Shift Keying (FSK) by changing the frequency of the carrier wave, helps reduce the bit error rate (BER) even in challenging conditions. For instance, Quadrature Phase Shift Keying (QPSK) modulation performs well over underwater-air links when combined with AO. For example, QPSK modulation achieves an effective apparent error rate (SER) in underwater-air links when paired with AO [7]. Recent advancements, like 100 Gbit/s multimode orbital angular momentum (OAM) transmission, show the promise of combining different methods. The third category includes a phase screen and computational methods. Wave front sensor configuration [8] and random phase screen (RPS) modeling [9] have emerged as cost-effective alternatives to hardware-intensive AO. The simulation process was used to address amplitude and phase distortions by constructing a turbulence model using the random phase screen approach. However, their impact on reducing the signal error rate (SER) in practical free-space optical (FSO) systems remains under investigation. Most studies have focused on improving BER or on using AO for phase correction. Still, few address optimizing SER for signals affected by disturbances, as well as low-cost solutions (like RPS) that balance performance and expense.

Several studies published over the past few years have demonstrated the impact of atmospheric disturbances on the propagation of light beams [10–12]. The major aim of the presented study is reducing the symbol error rate in atmospheric optical communication channels by adjusting the beam's mathematical parameters, rather than using expensive optical systems. The research offers a new perspective by focusing on improving SER through adjustments to the LG beam parameters rather than relying on complex corrective systems, opening a direct path to developing more efficient and less expensive technologies in optical communications.

Thus, this paper evaluates the SER performance of an optimized FSO system utilizing the random phase screen (RPS) method. Contrary to earlier research, we measure the extent to which the RPS method reduces the signal error rate (SER) under different turbulent conditions, compare its performance to

* Corresponding author: Asmaa M. Aubaid (asithmuh@mohesr.edu.iq).

traditional adaptive optics (AO) and modulation methods, and offer guidance on using RPS in budget-friendly FSO setups. The structure of the article is arranged as follows. Section 2 presents the theoretical aspect of the work, including descriptions of the vortex Laguerre beam's expression and the field intensity at the transmitter and receiver. Section 3 presents the calculation results with a discussion, and Section 4 provides the conclusion of this work.

2. THE THEORY

In this section, some theoretical terms and scientific models related to optical communication techniques will be explained, including beam types, transmitters, channel models, and receivers.

2.1. Expression of Vortex Laguerre Beam

The Laguerre polynomial is considered a mathematical function that represents solutions to specific differential equations. It is used in several fields of mathematics, including signal processing, mathematical fields, and linear systems analysis. It plays an effective role in optical communications by improving system performance through increased signal-to-noise ratio (SNR) and reduced SER, which is the focus of this study. This, in turn, leads to improved signal quality, which in turn improves transmission system performance.

In this section, we present a Laguerre vortex beam and evaluate its correction amplitude and SER performance in strong turbulence. A radial coordinate is used to define this beam, i.e., $(s, \emptyset)$. Among different types of optical vortex beams, the Laguerre-Gaussian mode is the most frequently referenced in the literature [13, 14]. Its mathematical form is typically expressed as:

$$u(s,\emptyset) = \left(\frac{s}{\propto_s}\right)^m \exp\left(-\frac{s^2}{\propto_s^2}\right) L_n^m\left(\frac{s^2}{\propto_s^2}\right) \exp(jm\emptyset) \quad (1)$$

where (s_x, s_y) are the transverse source plane coordinates, $s = s_x^2 + s_y^2$, and $u(s, \emptyset)$ will become plainly truncated because of the limited dimensions of the source plane. Thus, L_n^m corresponds to a Laguerre polynomial, where (n) denotes the order or degree of the polynomial function (radial index that affects the number of intensity rings); $\propto_s$ is the waist radius of a Gaussian beam; (m) represents the topological charge of the optical vortex. The radial index affects a beam's behavior under certain conditions, such as its ability to withstand turbulence and to rebuild itself after being blocked or scattered.

In summary:

- The radial intensity of a Laguerre-Gauss (LG) beam is determined by its radial index (n), which in turn controls the number of the beam's concentric rings. Then, the radial index affects the behavior of a beam under certain conditions, such as its ability to withstand turbulence and its ability to rebuild itself after being blocked or scattered, so it is important to increase the value of (n) in strong turbulence. On the other hand, the radial index (n) of the LGVB should be increased to reduce the symbol error rate (SER), thereby improving the performance regarding the optical transmission system, especially with the presence of atmospheric turbulence. Therefore, higher refractive indices lead to greater self-reconstruction capability and signal strength, thereby enhancing the performance related to the optical communication system [15].

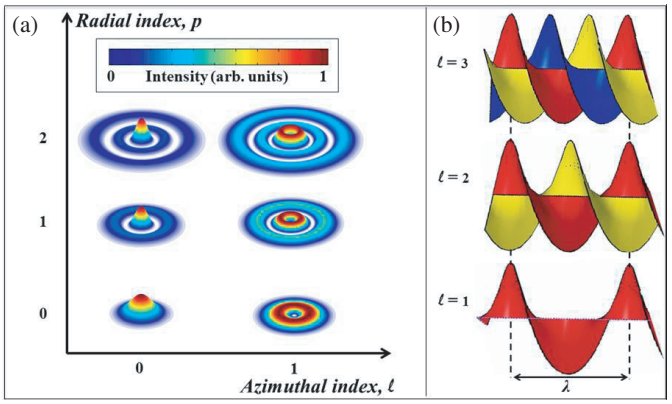

FIGURE 1. Laguerre-Gaussian (LG) beams, where (a) a two-dimensional light intensity diagram shows LG beams with various mode indices. The rows and columns represent the mode indices in their azimuthal and radial forms, respectively. (b) The helical wave front of LG beams is shown with an azimuthal index that varies from $(m = 1$ to $3)$ while the radial index is kept at zero $(n = 0)$ [16].

- The "azimuthal of Laguerre" can be more precisely described as the azimuthal component of mathematical solutions involving associated Laguerre polynomials, where this angle determines the orbital angular momentum (OAM) of a system. However, the azimuthal component causes a helical phase change of the light beam along the wavefront; for example, when $m = 4$, the phase changes by 8π around the axis. However, when $m = 0$, there is no angular phase, the beam is a normal Gaussian beam with no phase rotation. Fig. 1 shows Laguerre-Gaussian (LG) beams with two modes, explaining the azimuthal and radial indices [16].

$$L_n^m(r,\emptyset,z) = \frac{\propto_s}{\omega(z)} \exp\left(\frac{izr^2}{z_0\omega(z)^2} + i(2n+m+1)\gamma(z)\right) L_n^m\left(\frac{\omega r}{\omega(z)}, \emptyset,\right) \quad (2)$$

where $\omega(z) = \omega[1 + (\frac{z}{z_0})^2]^{1/2}$; $\gamma(z) = \arctan(z/z_0)$; $\gamma(z)$ represents the Gough phase; z_0 represents a Rayleigh range; and k represents the wavenumber of light [17].

- The effect of the azimuth index (m) (or topological loading) on the radiation emission rate (SER) in orbital angular momentum (OAM)-based optical communication systems.

- In optical division multiplexing (OAM) systems, information is encoded into packets with different values of (m)

(i.e., each value of (m) represents an independent channel). Each phase of type (exp $(jm\emptyset)$) in Equation (1) represents a distinct mode that can be used to transmit independent data. This results in greater capacity, as several modes of (m) can be used in parallel. The higher the value of (m), the greater the beam's sensitivity to angular disturbances, and, consequently, the higher the SER. Therefore, in our research to reduce the SER, we aim for the lowest possible value of (m).

2.2. Amplitude Field Mode

$u_{rt}(r_x, r_y, L)$ represents the received field of a beam that has traveled through air turbulence over a distance can be represented according to the Rytov theory [14]. Consequently, the analytical expression for the average intensity of a Laguerre beam propagating through a turbulent atmosphere is formulated by employing the extended Huygens-Fresnel diffraction integral in conjunction with the Rytov approximation and by using the random phase screen with the Kolmogorov model, to check the behavior of the beam in weak and strong turbulence.

$$u_{rt}(r_x, r_y, L) = u_{rfs}(r_x, r_y, L) \exp\left[\Psi\left(r_x, r_y, L\right)\right] \quad (3)$$

Here, (r_x, r_y) denote the transverse coordinates at the receiver plane, while $u_{rfs}(r_x, r_y, L)$, represents the free-space propagating field. The influence of atmospheric turbulence is incorporated into the complex phase function (r_x, r_y, L), which itself can be further decomposed into distinct components.

$$\Psi\left(r_x, r_y, L\right) = \Psi_r\left(r_x, r_y, L\right) + j\Psi_i(r_x, r_y, L) \quad (4)$$

Intensity fluctuations create scintillation at the receiver. By using Equations (3) and (4), the intensity on the received side $I_{rt}(r_x, r_y, L)$ becomes

$$\begin{aligned} I_{rt}\left(r_x, r_y, L\right) &= u_{rt}\left(r_x, r_y, L\right) u^*_{rt}\left(r_x, r_y, L\right) \\ &= u_{rfs}\left(r_x, r_y, L\right) u^*_{rfs}\left(r_x, r_y, L\right) \\ &\quad \exp\left[2\Psi_r\left(r_x, r_y, L\right)\right] \\ &= I_{rfs}\left(r_x, r_y, L\right) \exp\left[2\Psi_r\left(r_x, r_y, L\right)\right] \quad (5) \end{aligned}$$

where the intensity in open space is denoted by $I_{rfs}(r_x, r_y, L)$.

Equation (5) indicates that the fluctuations in the intensity function $I_{rt}(r_x, r_y, L)$ arise exclusively from the real component of the complex phase term, which can be expressed as

$$\Psi_r\left(r_x, r_y, L\right) = 0.5 \ln\left[\frac{I_{rt}(r_x + r_y + L}{I_{rfs}(r_x + r_y + L}\right] \quad (6)$$

It is easier for a receiver to evaluate $I_{rfs}(r_x, r_y, L)$ from the known analytical formulations for an optical communication system operating at a fixed distance of (L) and a known transmitted beam.

In the meantime, $I_{rt}(r_x, r_y, L)$ is the received intensity at turbulence.

2.3. The Modulation Technique

In our simulations, the constellation layout of the 4ASK modulation technique is depicted in Fig. 2. The symbol endpoints of the signal vectors are uniformly spaced by the optical power,

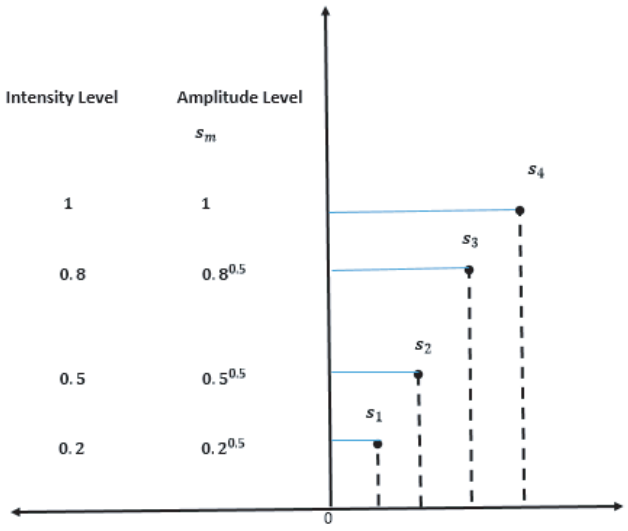

FIGURE 2. Explain a plane source for a 4ASK signal vector constellation.

with a maximum amplitude of 1 and a minimum of 0 for the normalized vectors. This study selects a vortex Laguerre beam as the source beam, with its field expression provided in Equation (1). The source beam will change when one of the 4ASK constellation's signal vectors modulates it:

$$u(s, \emptyset) = s_m * \left(\frac{s}{\propto_s}\right)^m \exp\left(-\frac{s^2}{\propto_s^2}\right) L_n^m\left(\frac{s^2}{\propto_s^2}\right) \exp\left(jm\emptyset\right) \quad (7)$$

where

$$s_m = \{s_1, s_2, s_3, s_4\} = \left\{0.2^{0.5}, 0.5^{0.5}, 0.8^{0.5}, 1\right\}$$

In this case, the separation between the terminal points of the signal vectors (symbols) is adjusted to be uniform in optical power. The minimum normalized signal vector corresponds to an amplitude level of $0.2^{0.5}$ whereas the maximum signal vector is assigned an amplitude level of unity. It should be noted that this unity level also represents the peak transmitted power under amplitude shift keying (ASK) modulation, and the condition is fulfilled when

$$s_m = s_{m4} = 1.$$

2.4. Configuration of Random Phase Screen Parameters

In constructing a random phase screen, the primary considerations are the grid interval and the number of sampling points (Ng) assigned to each rectangular dimension of the transverse plane at both the source and the receiver. Together, these two factors govern the spatial resolution achievable in the receiver plane and establish the observation constraints associated with the transmitter plane. The diffractive beam characteristics, the turbulence-induced spreading in the propagation medium, and the source beam profile all influence the choice of grid spacing and the number of grid factors. This operation also determines the number of intermediate-phase screen plates to be positioned between the receiver and transmitter; for further details on these calculations and limitations, refer to [17–19]. In ap-

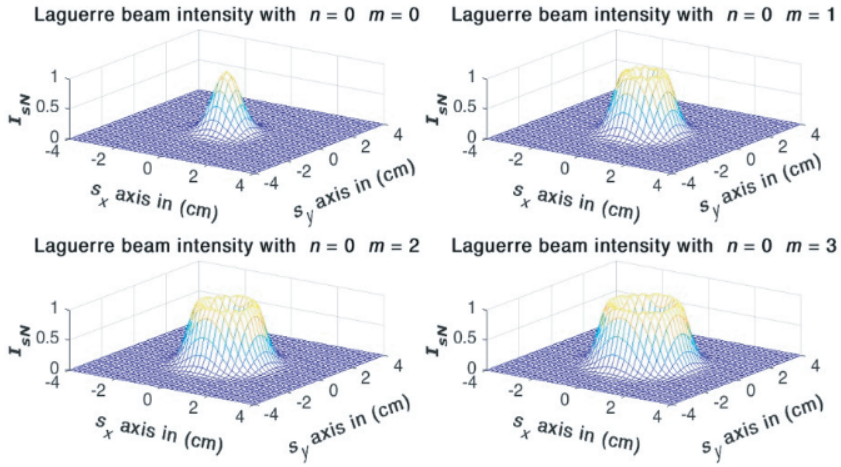

FIGURE 3. A three-dimensional view of source plane intensities of Vortex Laguerre Beam with $n = 0$, and $m = 0$, 1, 2, and 3.

plications involving RPS, the usual practice is to represent Ng as a power of 2. In this study, Ng is established at 512, with a wavelength range of 1550 nm. This indicates that achieving an average result sufficiently close to the theoretical limits of the analytical model requires maintaining a large value of Ng, representing the number of runs. However, increasing Ng inevitably increases computational time, making the process progressively more resource-intensive. Testing indicated that Ng $= 500$ is an appropriate choice, consistent with values reported in the literature [17, 19]. The numerical outcomes of this work were obtained by establishing ($\propto_s =$ 1 cm) and considering the source as well as propagation circumstances, leading to the implementation of a suitable RPS model. To ensure result reliability, measures are implemented to ensure that the RPS arrangement withstands severe turbulence. The 4ASK broadcasts have a 3 km propagation distance, a 1550 nm wavelength, and a structure constant [SC] that is varied between $10^{-15}\,\mathrm{m}^{-2/3}$ and $10^{-13}\,\mathrm{m}^{-2/3}$.

Given these numerical values, it can be readily demonstrated that the proposed system maintains effective performance even under strong turbulence conditions, while fully satisfying the constraints specified in [20, 21]. A Stability Switching (SSC) integration diversity scheme operating over a fading channel is discussed. Then, the evaluated results for the respective channel parameters are plotted, and the effect of fading intensity is observed [22]. The bit error rate (BER) values were calculated for the corresponding signal-to-noise ratio (SNR) to determine the various scattering effects in non-line-of-sight propagation of the UWAC system [23].

3. RESULTS AND DISCUSSIONS

In the present section, the findings obtained through this study will be reviewed, discussed, and compared with other studies.

3.1. Results of Source Plane Intensities of Vortex Laguerre Beams

This section discusses how the parameters of the Laguerre polynomial influence the distribution of free-space source intensities. Initially, the parameter (n) was assigned constant values of (0, 1, 2, and 3) for each considered case, while the parameter (m) was varied independently, also taking the values (0, 1, 2, and 3) for each corresponding scenario. The following figures show the impact of Laguerre polynomial parameters on source intensity to get different cases of SER when ($n = 0$) with ($m = 0$, 1, 2, and 3) and ($n = 3$) with ($m = 0$, 1, 2, and 3). On the other side, when ($m = 0$) with ($n = 0$, 1, 2, and 3) and ($m = 3$) with ($n = 0$, 1, 2, and 3), at the end ($n = 0$, 1, 2, and 3) with ($m = 0$, 1, 2, and 3). The view of the transmitter plane intensities of the Vortex Laguerre Beam with chosen values of the Laguerre polynomial parameters can be observed in Figs. 3, 4, 5, and 6, respectively. However, the values of the source intensity against the x-y axis can be seen clearly in Figs. 4, 5, and 6 for a constant value of (n) but with a variety of (m) parameter values, which means that they will be a difficult-to-recognize receiving signal on the detector side.

However, when ($n = 3$, $m = 1$), ($n = 2$, $m = 1$), ($n = 1$, $m = 0$), and ($n = 0$, $m = 0$), it is indicated that the source-intensity values along the x-y axis are clearly spaced because they will be an easy-to-recognize receiving signal on the detector side (see Figure 7) and yield suitable results for SER.

3.2. SER Results

The SER is a measure that determines the number of errors that occur with receiving symbols relative to the number of symbols transmitted through the channel. Therefore, it is an important factor in evaluating system performance. This article focuses on the SER and seeks to reduce it to achieve optimal performance in optical communication systems.

This section presents the outcomes of SER evaluations. As evidenced from Fig. 7 to Fig. 11, the discrepancies in SC values from $C_n^2 = 10^{-13} - 10^{-15} m^{-2/3}$, in the unstable environment, where the 4ASK signals have been relayed, significantly affect SER.

In these figures, it is found that the graphs of SER are plotted against the structure constant (C_n^2), where a difference in values of C_n^2, it was created. After that, it became clear that SER would spike sharply during periods of intense disturbance. It is evident

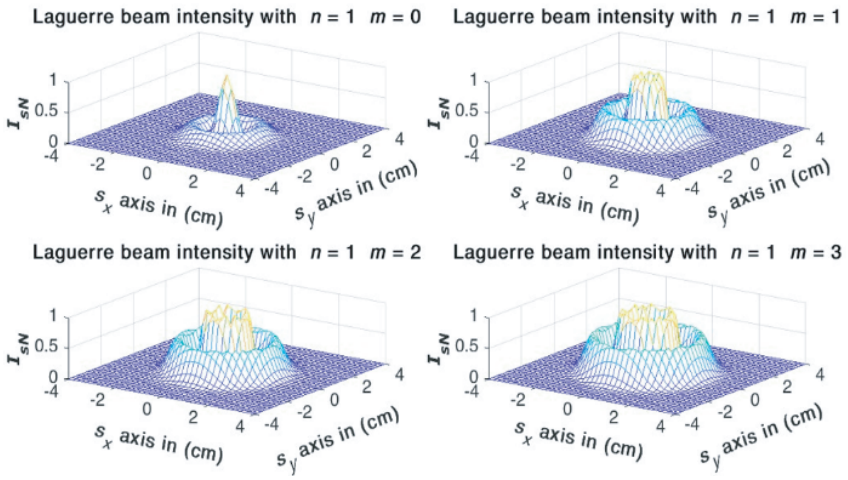

FIGURE 4. Three-dimensional representation of the source-plane intensity distribution for a Vortex Laguerre Beam with $(n = 1)$ and $(m = 0, 1, 2)$ and (3).

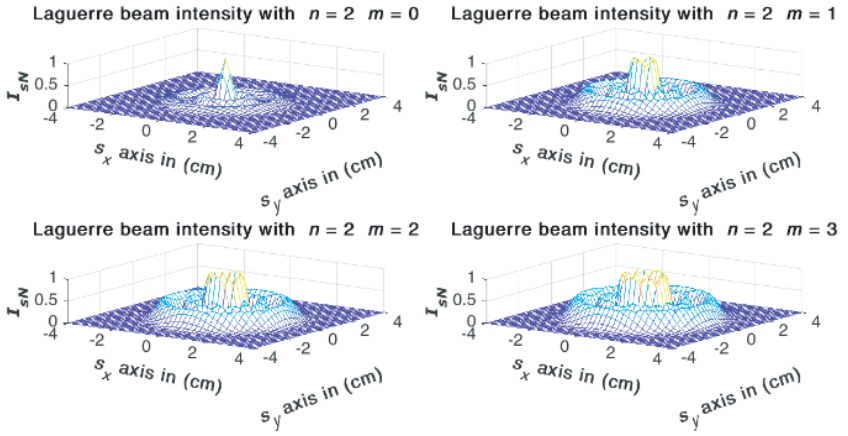

FIGURE 5. Three-dimensional illustration of the source-plane intensity distribution for a Vortex Laguerre Beam with $(n = 2)$ and $(m = 0, 1, 2)$ and (3).

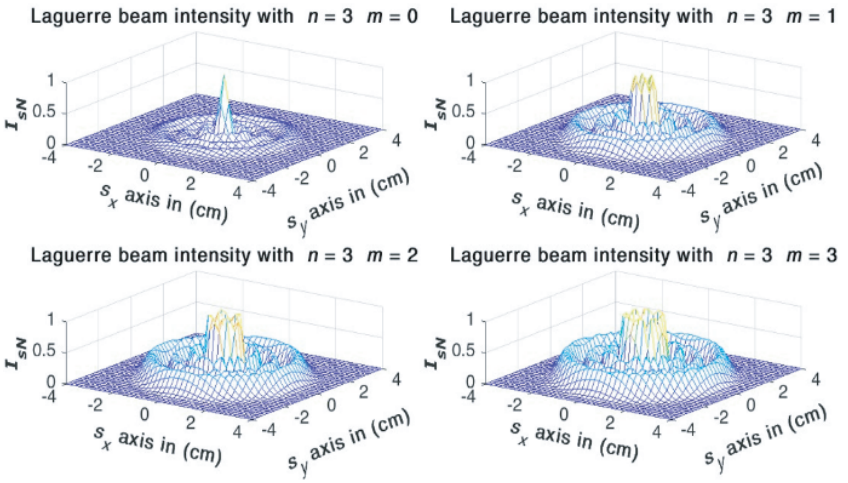

FIGURE 6. Three-dimensional illustration of the source-plane intensity distribution for a Vortex Laguerre Beam with $(n = 3)$ and $(m = 0, 1, 2)$ and (3).

that under the given conditions ($n = 0$, $m = 0$, and $n = 0$, $m = 1$), the behavior of SER is more favorable than under the conditions ($n = 0$, $m = 2$, and $n = 0$, $m = 3$); this is illustrated in Fig. 8. In the same way, if the value of SC were to change, as shown in Fig. 9, SER would rise rapidly once again. In addition, for setting Laguerre polynomial parameters for the following ($n = 1$, $m = 3$, and $n = 1$, $m = 2$), but the behavior of SER is better in cases of ($n = 1, m = 0$, and $n = 1$, $m = 1$), and in the same way in Figs. 10 and 11, respectively. Finally, it appears from Fig. 12 that when Laguerre polynomial

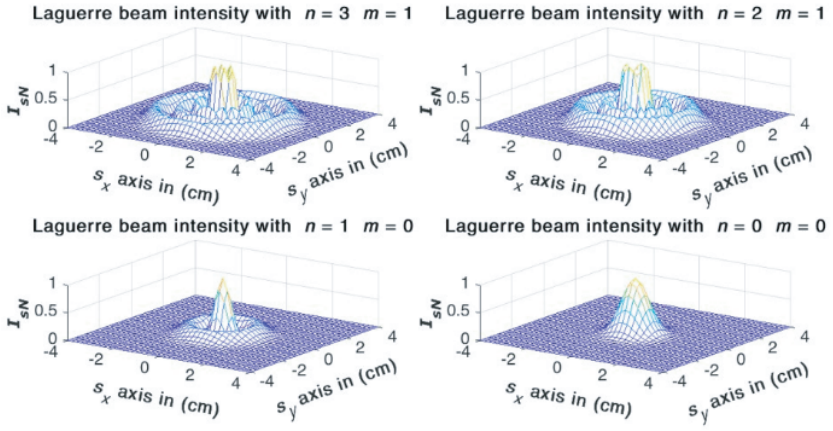

FIGURE 7. Three-dimensional illustration of the source-plane intensity distributions for Vortex Laguerre Beams with parameter sets ($n = 3$, $m = 1$), ($n = 2$, $m = 1$), ($n = 1$, $m = 0$), and ($n = 0$, $m = 0$).

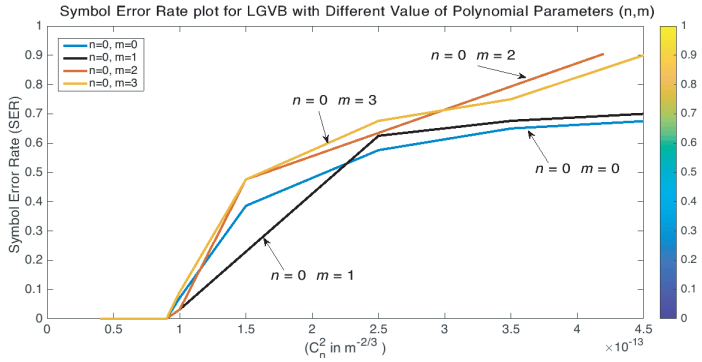

FIGURE 8. The effectiveness of changing the number of polynomials of LGVB on Symbol Error Rate SER with $n = 0$, and $m = 0$, 1, 2, and 3.

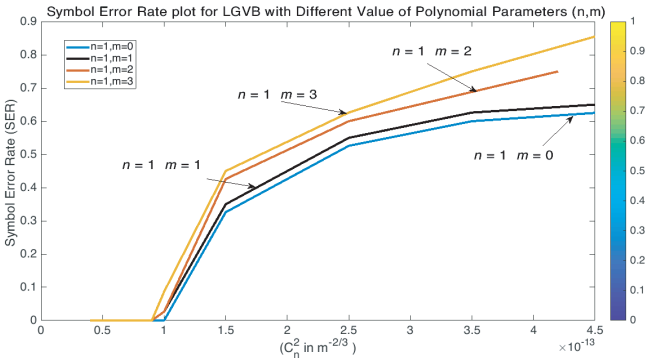

FIGURE 9. The effectiveness of changing the number of polynomials of LGVB on SER with $n = 1$, and $m = 0$, 1, 2, and 3.

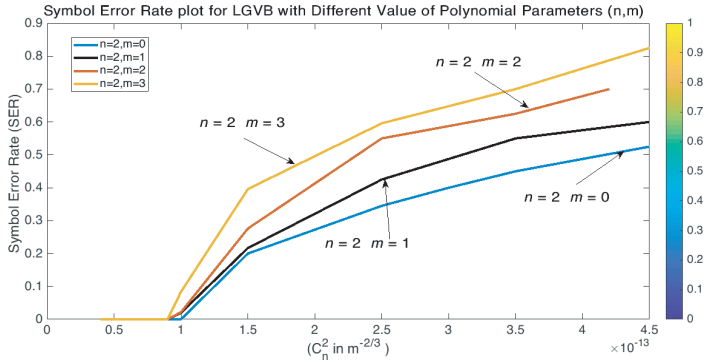

FIGURE 10. The effectiveness of changing the number of polynomials of LGVB on SER with $n = 2$, and $m = 0$, 1, 2, and 3.

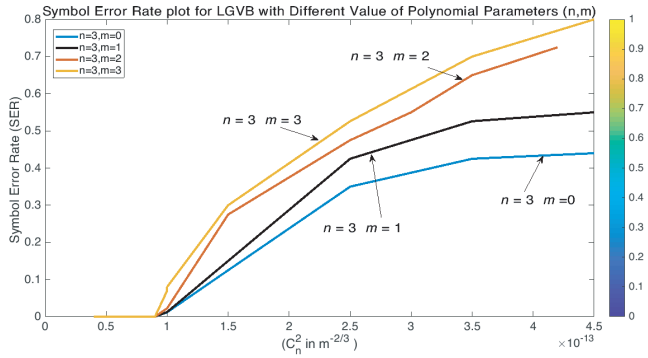

FIGURE 11. The effectiveness of changing the number of polynomials of LGVB on SER with $n = 3$, and $m = 0$, 1, 2, and 3.

parameters are set in the following SER ($n = 3$ with $m = 0$), ($n = 2$ with $m = 0$), ($n = 1$ with $m = 0$), and ($n = 0$ with $m = 0$), the SER will be good, especially when polynomial parameters are adjusted to ($n = 3$ with $m = 0$) and ($n = 2$ with $m = 0$).

According to the fact that the higher the value of (m), the greater the sensitivity of the beam to angular disturbances, and therefore the rate of radiation emission increases, and this in turn leads to an increase in (SER), and the opposite is true, i.e., to get the lowest possible (SER) in a turbulent atmosphere, we take the lowest possible (m), which is (m: $m = 0$). On the other hand, to obtain a low symbol error rate (SER), a high refractive index (n) is chosen for the Laguerre-Gaussian vortex beam, corresponding to the highest value obtained in these results ($n = 3$). This, in turn, improves the performance of the optical transmission system in a turbulent environment.

Our results are compared with previous studies that used a Laguerre-based polynomial to obtain the superposition of coherent light, which became particularly relevant to optical communications with the advent of optical amplifiers, as in [24].

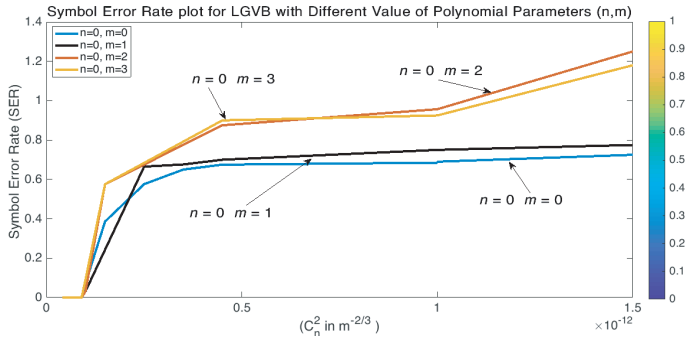

FIGURE 12. The effectiveness of changing the number of polynomials of LGVB on SER with $n = 0$, and $m = 0$, 1, 2, and 3, in moderate and high turbulence.

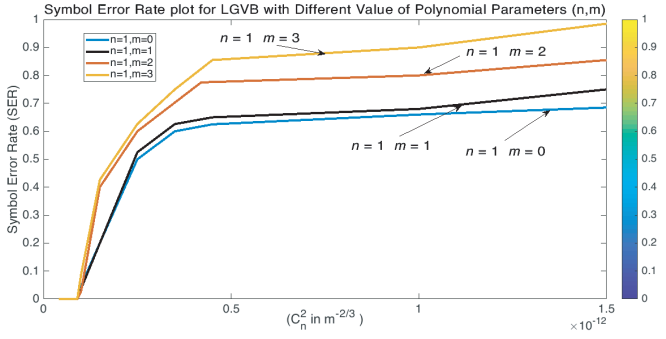

FIGURE 13. The effectiveness of changing the number of polynomials of LGVB on SER with $n = 1$, and $m = 0$, 1, 2, and 3, in moderate and high turbulence.

TABLE 1. Symbol error rate of LGVB with the number of polynomials $n = 0$, and $m = 0$, 1, 2, and 3.

C_n^2	SER ($n = 0, m = 0$)	SER ($n = 0, m = 1$)	SER ($n = 0, m = 2$)	SER ($n = 0, m = 3$)
4E-14	0	0	0	0
7E-14	0	0	0	0
8E-14	0	0	0	0
9E-14	0	0	0	0
1E-13	0.0717	0.03167	0.03167	0.09111
2.5E-13	0.386	0.625	0.476	0.476
3.5E-13	0.576	0.676	0.905	0.676
4.5E-13	0.65	0.7		0.75

TABLE 2. Symbol Error Rate SER of LGVB with the number of polynomials $n = 1$, and $m = 0$, 1, 2, and 3.

C_n^2	SER ($n = 1, m = 0$)	SER ($n = 1, m = 1$)	SER ($n = 1, m = 2$)	SER ($n = 1, m = 3$)
4E-14	0	0	0	0
7E-14		0	0	0
8E-14	0	0	0	0
9E-14	0	0	0 0.02667	0
1E-13	0	0.02667	0.426	0.08667
2.5E-13	0.326	0.35	0.6	0.45
3.5E-13	0.526	0.55		0.626
4.5E-13	0.6	0.626	0.8	0.75

TABLE 3. Symbol Error Rate SER of LGVB with the number of polynomials $n = 2$, and $m = 0$, 1, 2, and 3.

C_n^2	SER ($n = 2, m = 0$)	SER ($n = 2, m = 1$)	SER ($n = 2, m = 2$)	SER ($n = 2, m = 3$)
4E-14	0	0	0	0
7E-14	0	0	0	0
8E-14	0	0	0	0
9E-14	0	0	0	0
1E-13	0	0.02	0.02167	0.08367
1.5E-13	0.2	0.2167	0.276	0.396
2.5E-13	0.345	0.425	0.55	0.596
3.5E-13	0.45	0.55	0.625	0.7
4.5E-13	0.525	0.6		0.825

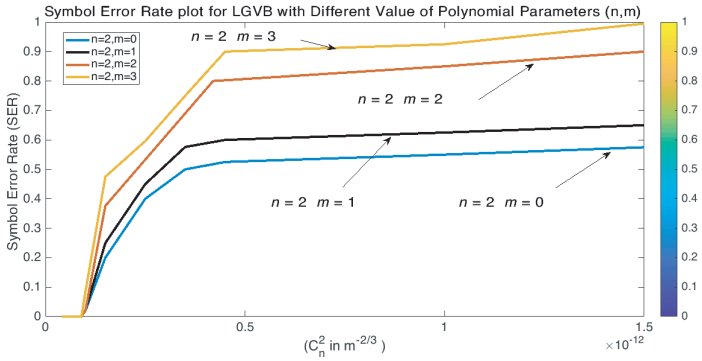

FIGURE 14. The effectiveness of changing the number of polynomials of LGVB on SER with $n = 2$, and $m = 0$, 1, 2, and 3, in moderate and high turbulence.

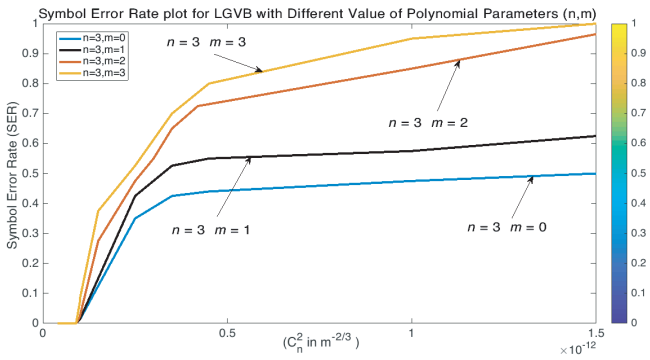

FIGURE 15. The effectiveness of changing the number of polynomials of LGVB on SER with $n = 3$, and $m = 0$, 1, 2, and 3, in moderate and high turbulence.

TABLE 4. Symbol Error Rate SER of LGVB with the number of polynomials $n = 3$, and $m = 0$, 1, 2, and 3.

C_n^2	SER ($n = 3, m = 0$)	SER ($n = 3, m = 1$)	SER ($n = 3, m = 2$)	SER ($n = 3, m = 3$)
4E-14	0	0	0	0
7E-14	0	0	0	0
8E-14	0	0	0	0
9E-14	0	0	0	0.07
1E-13	0.12	0	0.2267	0.08
1.5E-13	0.125	0.01267	0.275	0.3
2.5E-13	0.35	0.425	0.475	0.526
3.5E-13	0.425	0.526	0.65	0.7
4.5E-13	0.44	0.425		0.8

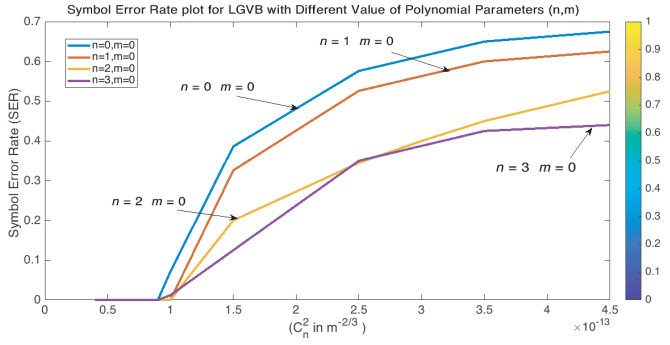

FIGURE 16. The effectiveness of changing the number of polynomials of LGVB on SER ($n = 3$ with $m = 0$), ($n = 2$ with $m = 0$), ($n = 1$ with $m = 0$), and ($n = 0$ with $m = 0$) into weak and moderate turbulence.

Our study is also compared with other studies, such as Pengfei Y and et al., they presented SER performance of the Underwater Wireless Optical Communication System (UWOC) was investigated using a composite generalized exponential gamma (EGG) distribution with a beam spread function (BSF) under two difficult decision schemes for a fixed decision threshold (FDT) and a dynamic decision threshold (DDT). Using the Gauss-Laguerre quadratic function, the analytical SER expressions for these two threshold schemes were derived and validated via Monte Carlo (MC) simulation [25]. Table 1 & Figure 8 show the effectiveness of changing the number of polynomials of LGVB on SER with $n = 1$, and $m = 0$, 1, 2, and 3.

Tables 2, 3 & Figs. 9 and 10 explain the effectiveness of changing the number of polynomials of LGVB on SER with $n = 1$, and $m = 0$, 1, 2, and 3; $n = 2$, and $m = 0$, 1, 2, and 3.

Finally, Table 4 & Fig. 11 introduce the effectiveness of changing the number of polynomials of LGVB on SER with $n = 3$, and $m = 0$, 1, 2, and 3.

Figure 11 introduces the effectiveness of changing the number of polynomials of LGVB on SER with $n = 3$ and $m = 0$, 1, 2, and 3.

4. CONCLUSION

A simulation study of the symbol error rate (SER) was carried out, in which the influence of altering the structural constant was systematically investigated within a specified range $C_n^2 = 10^{-15}$ to $10^{-12}m^{-2/3}$, which is represented as the values of turbulence. By varying multiple parameters in LGVB and across different SC values and turbulence conditions (weak, medium, strong), the symbol error rate was examined. Subsequently, it is demonstrated that variations in polynomial parameter values significantly influence the behavior of SER and the

intensity profile of the LGVB. Even for deviations in the structural constant's value, SER would rise quickly, especially under strong turbulence. The alteration of polynomial parameters in LGVB is attributed to an increase in SER, particularly when the changeable polynomial parameters are set to specific values. For example, the polynomial parameters have been set to (a) $n = 0$, and $m = 0$, 1, 2, and 3; (b) $n = 1$, and $m = 0$, 1, 2, and 3; (c) $n = 2$, and $m = 0$, 1, 2, and 3; (d) $n = 3$, and $m = 0$, 1, 2, and 3. Then, the deviations of SC values from (10^{-16}) to (10^{-12}), for each case represent the turbulence of the atmosphere from weak, moderate to strong values. In the previous cases, the results showed that the spread of LVGB at $(n = 3, m = 0)$ spreads more quickly on LVGB with packages $(n = 2, m = 0)$, $(n = 1, m = 0)$, and $(n = 0, m = 0)$ for stronger disorder and smaller values (SER). Finally, LVGB with polynomial parameters $(n = 3, m = 0)$ is the best in terms of SER (lowest) among the polynomial parameters. However, to clarify the effect of the turbulences more clearly on SER, it is focused on medium and strong of turbulence values, i.e., SC, with values limited between (10^{-16}) and (10^{-12}), as shown in Figs. 12, 13, 14, 15, and 16, which give documented results that $(n = 3, m = 0)$ is the best and more appropriate in choice than other combinations of polynomial parameters. Most previous studies have focused on improving SER using adaptive optics or modulation. In contrast, a novel approach was used here, which focuses on creating a simulation that mimics a carrier optical medium in which the turbulence varies from weak to moderate to strong. The results showed a high degree of agreement with the mathematical analysis of the Lager polynomial. Finally, this work is distinguished by its introduction of an innovative approach that relies on choosing (n, m) parameters as an effective tool to improve the performance of LG beams under disturbance, a trend that previous research has not given its due attention despite its high importance in free optical communications.

To conclude, the outcomes of this study indicate that the Laguerre Vortex Gaussian Beam (LVGB) with parameters $(n = 3, m = 0)$ offers promising prospects for applications in remote sensing, as well as free-space optical communication systems. This configuration exhibited stable and enhanced performance under strong turbulence conditions compared to other beam structures characterized by different (n, m) values.

REFERENCES

[1] Tyson, R. K., "Using the deformable mirror as a spatial filter: Application to circular beams," *Applied Optics*, Vol. 21, No. 5, 787–793, 1982.

[2] Andrews, L. C. and R. L. Phillips, *Laser Beam Propagation through Random Media*, 2nd ed., SPIE Press, 2005.

[3] Mackey, R. and C. Dainty, "Wavefront sensing and adaptive optics in strong turbulence," in *Opto-Ireland 2005: Photonic Engineering*, Vol. 5827, 23–29, Dublin, Ireland, 2005.

[4] Schwartz, N. H., N. Védrenne, V. Michau, M.-T. Velluet, and F. Chazallet, "Mitigation of atmospheric effects by adaptive optics for free-space optical communications," in *Atmospheric Propagation of Electromagnetic Waves III*, Vol. 7200, 133–143, San Jose, California, United States, 2009.

[5] Stotts, L. B., P. Kolodzy, A. Pike, B. Graves, D. Dougherty, and J. Douglass, "Free-space optical communications link budget estimation," *Applied Optics*, Vol. 49, No. 28, 5333–5343, 2010.

[6] Sharma, S., "A simplified free-space adaptive optics system against atmospheric turbulence," *International Journal of Electronics*, Vol. 99, No. 3, 417–436, 2012.

[7] Li, M. and M. Cvijetic, "Coherent free space optics communications over the maritime atmosphere with use of adaptive optics for beam wavefront correction," *Applied Optics*, Vol. 54, No. 6, 1453–1462, 2015.

[8] Sergeyev, A. V., E. Levin, and M. C. Roggemann, "Wavefront sensor alignment and calibration techniques for laser communication systems," in *Cyber Sensing 2012*, Vol. 8408, 242–250, Baltimore, Maryland, United States, 2012.

[9] Gregory, M., D. Troendle, G. Muehlnikel, F. Heine, R. Meyer, M. Lutzer, and R. Czichy, "Three years coherent space to ground links: Performance results and outlook for the optical ground station equipped with adaptive optics," in *Free-Space Laser Communication and Atmospheric Propagation XXV*, Vol. 8610, 17–29, San Francisco, California, United States, 2013.

[10] Nossir, N., L. Dalil-Essakali, and A. Belafhal, "Behavior of the central intensity of generalized Humbert-Gaussian beams against the atmospheric turbulence," *Optical and Quantum Electronics*, Vol. 53, No. 12, 665, 2021.

[11] Hricha, Z., M. Lazrek, M. E. Halba, and A. Belafhal, "Effect of a turbulent atmosphere on the propagation properties of partially coherent vortex cosine-hyperbolic-Gaussian beams," *Optical and Quantum Electronics*, Vol. 54, No. 11, 719, 2022.

[12] Ebrahim, A. A. A., M. A. Swillam, and A. Belafhal, "Atmospheric turbulent effects on the propagation properties of a general model vortex higher-order cosh-Gaussian beam," *Optical and Quantum Electronics*, Vol. 55, No. 4, 316, 2023.

[13] Cheng, W., J. W. Haus, and Q. Zhan, "Propagation of scalar and vector vortex beams through turbulent atmosphere," in *Atmospheric Propagation of Electromagnetic Waves III*, Vol. 7200, 22–31, San Jose, California, United States, 2009.

[14] Eyyuboğlu, H. T., Y. Baykal, and A. Falits, "Scintillation behavior of Laguerre Gaussian beams in strong turbulence," *Applied Physics B*, Vol. 104, No. 4, 1001–1006, 2011.

[15] Wang, Y., L. Bai, J. Xie, C. Huang, and L. Guo, "Radial spectrum spread of Laguerre-Gaussian beam transmission in weak compressible turbulence," *Optics Communications*, Vol. 554, 130111, 2024.

[16] Mourka, A., "Probing the modal characteristics of novel beam shapes," Ph.D. dissertation, University of St Andrews, UK, 2013.

[17] Plick, W. N. and M. Krenn, "Physical meaning of the radial index of Laguerre-Gauss beams," *Physical Review A*, Vol. 92, No. 6, 063841, 2015.

[18] Johnston, R. A. and R. G. Lane, "Modeling scintillation from an aperiodic Kolmogorov phase screen," *Applied Optics*, Vol. 39, No. 26, 4761–4769, 2000.

[19] Belmonte, A., "Feasibility study for the simulation of beam propagation: Consideration of coherent lidar performance," *Applied Optics*, Vol. 39, No. 30, 5426–5445, 2000.

[20] Schmidt, J. D., *Numerical Simulation of Optical Wave Propagation with Examples in MATLAB*, SPIE Press, Bellingham, 2010.

[21] Voelz, D., *Computational Fourier Optics: A MATLAB Tutorial*, SPIE Press, Washington, 2011.

[22] Pranitha, B. and L. Anjaneyulu, "Performance evaluation of a MIMO based underwater communication system under fading conditions," *Engineering, Technology & Applied Science Research*, Vol. 9, No. 6, 4886–4892, Dec. 2019.

[23] Eyadeh, A. A. and M. N. Al-Ta'ani, "Performance study of wireless systems with switch and stay combining diversity over α-η-μ fading channels," *Engineering, Technology & Applied Science Research*, Vol. 9, No. 6, 5047–5055, Dec. 2019.

[24] Martinelli, M. and P. Martinelli, "Laguerre mathematics in optical communications," *Optics and Photonics News*, Vol. 19, No. 2, 30–35, 2008.

[25] Yang, P., W. Pang, S. Li, P. Wang, W. Chen, and H. Che, "SER performance investigation of UWOC system over composite EGG oceanic turbulence fading channel with BSF," *Optoelectronics Letters*, Vol. 18, No. 10, 606–612, 2022.